Fermi surface of the one-dimensional Hubbard model

C. Bourbonnais, H. Nélisse, A. Reid, and A.-M. S. Tremblay
Département de Physique et Centre de Recherche en Physique du Solide, Université de Sherbrooke, Sherbrooke, Québec, Canada J1K 2R1
(Received 1 March 1989)

Recent computer simulations performed on the one-dimensional Hubbard model with a new algorithm developed by Sorella *et al.* confirm the absence of a Fermi surface in this model at half filling. However, these same simulations suggest the existence of a Fermi surface at zero temperature away from half filling, contrary to expectations based on renormalization-group analysis. The results found here, using a more standard algorithm and a simple low-temperature extrapolation, appear consistent with the above-mentioned numerical results in the half-filled and quarter-filled band cases. However, it is argued that the discontinuity at the Fermi level found in all these simulations is likely to come from the zero-temperature finite-size dependence of the quasiparticle weight Z, which is also discussed here.

I. INTRODUCTION

High-temperature superconductivity has motivated renewed interest in the Hubbard model. In particular, one of the key questions is whether the two-dimensional Hubbard model away from half filling may be described by Fermi-liquid concepts, or if a whole new description with new kinds of elementary excitations is necessary. A popular tool to attack such questions is now computer simulations. To test the validity of this approach, it is advisable to first consider cases where we think the answer is known. It thus came as a surprise when Sorella, *et al.*,[1] using a new algorithm which allows them to go to much larger systems sizes and lower temperatures than previously possible, found a well-defined jump in the momentum distribution away from half filling. This result is the one expected for Fermi liquids, but it is in apparent contradiction with the one-dimensional zero-temperature renormalization-group prediction[2] that the momentum distribution is continuous with a power-law behavior around the Fermi wave vector. Even though the renormalization-group approach to the Hubbard model is approximate, it is believed to be accurate for not too strong coupling. We should also point out that despite the existence of the Lieb-Wu[3] exact solution to the one-dimensional Hubbard model, correlation functions are known in relatively few cases. In particular, the momentum distribution, to our knowledge, has been derived from the Lieb-Wu result only at half filling and in the limit of strong on-site repulsion.[4] In that special case there is definitely no jump in the momentum distribution at the Fermi wave vector, a result which the foregoing simulations did reproduce.

Since the algorithm of Sorella *et al.* is new, we thought it would be worthwhile to test their results with the better-tested algorithm of Blankenbecler, Scalapino, Sugar, and Hirsch (BSSH).[5] In one dimension, this algorithm is not as efficient as world-line methods,[6] but it is more easily generalizable to higher dimensions. Also, the BSSH algorithm is designed for the grand-canonical ensemble, whose convergence to the infinite-size limit is presumably different, and perhaps even faster, than that of the canonical ensemble.

The system we are studying is the one-dimensional Hubbard model

$$H=-t\sum_{\substack{\langle i,j\rangle\\ \sigma}}(c_{i\sigma}^{\dagger}c_{j\sigma}+c_{j\sigma}^{\dagger}c_{i\sigma})+U\sum_{i}n_{i_\uparrow}n_{i_\downarrow}-\mu\sum_{i,\sigma}n_{i\sigma}\ , \tag{1}$$

where σ is the spin label and $\langle i,j\rangle$ denotes a sum over nearest neighbors on a one-dimensional lattice. We use periodic boundary conditions and consider the case $U/t=4$ with average site occupation $\rho=1$, $\frac{30}{32}$, and $\frac{1}{2}$. Improvements of the BSSH algorithm allowing to go to very low temperatures were announced[7] after this work was completed. In the older form of the algorithm,[5] which we are using, we are, however, restricted to higher temperatures than were achievable by Sorella *et al.* Nevertheless, at half filling, we are apparently very close to the low-temperature limit so our results may be compared directly to theirs, while at quarter filling, a spectral weight analysis allows us to extrapolate our results to sufficiently low temperatures and to confirm theirs. For $\rho=\frac{30}{32}$, our results are inconclusive for reasons which are discussed in the text.

While our numerical results mostly confirm those of Sorella[1] *et al.*, we argue through renormalization-group arguments[2,8] that the jump seen in both sets of results is most likely to be a finite-size effect, even for the largest systems (200 sites) considered by Sorella *et al.* As we show here, this comes from the fact that at zero temperature, the size of the jump at the Fermi surface vanishes as a very small power law of the system size. In Sec. II, we describe our methodology. The results and their interpretation are in Sec. III. We conclude with additional discussion of the results.

II. DESCRIPTION OF THE METHOD, CHOICE OF PARAMETERS, SOURCES OF ERROR

All the results are for the one-dimensional Hubbard model with $t=1$, and $U=4$. The lattice spacing is unity, so that wave vectors are contained between $-\pi$ and π. As in Ref. 5, measurements are taken only every other full Monte Carlo sweep through the (1 + 1)-dimensional lattice. All our results are for 400 warmup sweeps and 500 measurements (1000 sweeps). Figure 1 illustrates the size dependence of the momentum distribution for $\rho=1$, $\beta=5$, $\Delta\tau=0.125$ (upper curve) and $\rho=\frac{1}{2}$, $\beta=7$, $\Delta\tau=0.20$ (lower curve). There is very little size dependence in the half-filled case, consistent with the idea that the localization length is very short in this regime. The absolute error on the momentum distribution coming from Monte Carlo sampling is, in this case, ± 0.03. There is a more important size dependence in the quarter-filled case $\rho=\frac{1}{2}$, but size $L=16$ is quite close to size $L=32$ except for one point. Nevertheless, comparing for $L=16$ and 32, the systematic error due to finite-size effects is within the Monte Carlo sampling accuracy. In this quarter-filled case, this sampling error depends on temperature and wave vector. It is largest at the lowest temperatures. For example, at $\beta=6$, the absolute sampling error varies from ± 0.17 at $k=0$ to ± 0.02 at $k=\pi$, while for $\beta=3.75$ it varies from ± 0.08 at $k=0$ to ± 0.01 at $k=\pi$.

The imaginary-time discretization is another source of systematic error which was analyzed in detail in Ref. 9 where it was in particular shown that, for the algorithm that we are using, it is of order $(\Delta\tau)^2$, where $\Delta\tau$ is the imaginary-time step. This is illustrated in Fig. 2 through a calculation of the kinetic and total energy for $L=16$, $\beta=5$, and various values of $\Delta\tau$. From these results we choose $\Delta\tau=0.125$ for $\rho=1$ (solid lines on Fig. 2). The systematic error in this case is at most 4%, which is of the same order as our Monte Carlo sampling error. A similar plot for $\rho=\frac{30}{32}$ dictates the same choice of $\Delta\tau$ for this band filling. For $\rho=\frac{1}{2}$ (dashed lines in Fig. 2), we choose $\Delta\tau=0.20$ with negligible systematic error. We also checked for this band filling and for $L=16$, $\beta=7$, and $L=32$, $\beta=4$ that this choice of $\Delta\tau$ leads to a systematic error for the momentum distribution itself which is well within our sampling error.

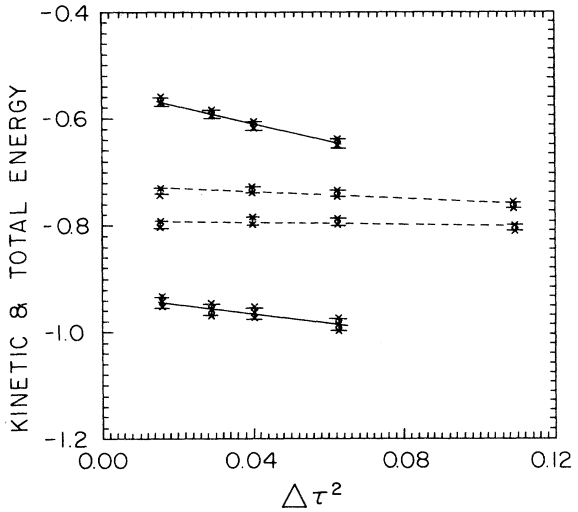

FIG. 2. Kinetic and total energy as a function of the square of the imaginary-time step $\Delta\tau^2$ for a chain of $L=16$ sites at $\beta=5$. Solid line is a least-squares fit to the half-filled ($\rho=1$) cases and dashed line is a least-squares fit to the quarter-filled ($\rho=\frac{1}{2}$) cases. The lowest lines are for kinetic energy, and the highest ones are for total energy. Error bars come from the Monte Carlo sampling.

We are interested in the limiting low-temperature behavior of the model. Figure 3 gives us an indication of

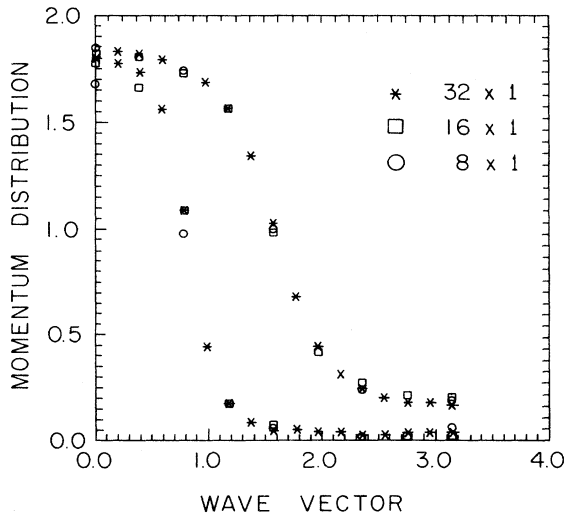

FIG. 1. Size dependence of the momentum distribution. $t=1$, $U=4$, asterisk, 32 sites; square, 16 sites; circles, 8 sites. Upper curve, $\rho=1$, $\beta=5$, $\Delta\tau=0.125$; lower curve, $\rho=\frac{1}{2}$, $\beta=7$, $\Delta\tau=0.20$.

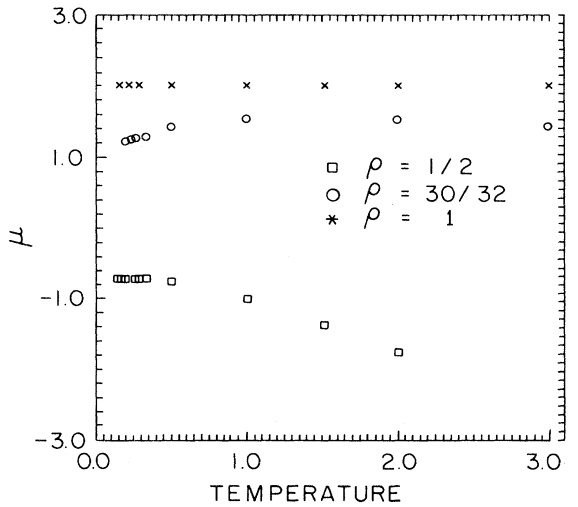

FIG. 3. Temperature dependence of the chemical potential for $L=32$, $\rho=1$ (crosses), $\rho=\frac{30}{32}$ (circles), and $\rho=\frac{1}{2}$ (squares). $t=1$, $U=4$, while $\Delta\tau=0.125$ for the first two band fillings, and $\Delta\tau=0.20$ in the last one.

this limit, at least in the quarter-filled $\rho=\frac{1}{2}$ case. There we see that for $\beta>3$ ($T<\frac{1}{3}$), the chemical potential saturates towards its low-temperature value. We take this as an indication that if a zero-temperature quasiparticle picture holds for the interacting system, this is the regime where it does. That the chemical potential is an indication of that fact can also be seen at the opposite high-temperature limit $\beta<\frac{1}{3}$, $T>3$, where we find, for $\rho=\frac{1}{2}$, both that the chemical potential is very near the free-electron value and that the momentum distribution becomes nearly identical with the free-electron result. We note in passing that, except in the half-filled case, the chemical potential has to be determined from the desired band filling using a Newton procedure. We obtained the desired band fillings to within an uncertainty of about 0.6%, which is much smaller than the sampling error on other quantities. Another indication that our lowest temperatures are close enough to the zero-temperature result comes from the value of the kinetic and total energy obtained in Fig. 2. The extrapolated finite-temperature $\beta=5$, $\Delta\tau=0$ results are at most 6% larger than the exact zero-temperature values[1,3] for $\rho=1$ and $\frac{30}{32}$.

III. RESULTS

Figures 4(a)–4(c) are our main raw results. They represent the momentum distribution for various band fillings in the low-temperature limit just defined. Also shown with squares are the results of Ref. 1 for $\rho=1$, and $\frac{30}{32}$. The first observation is that there is a temperature-

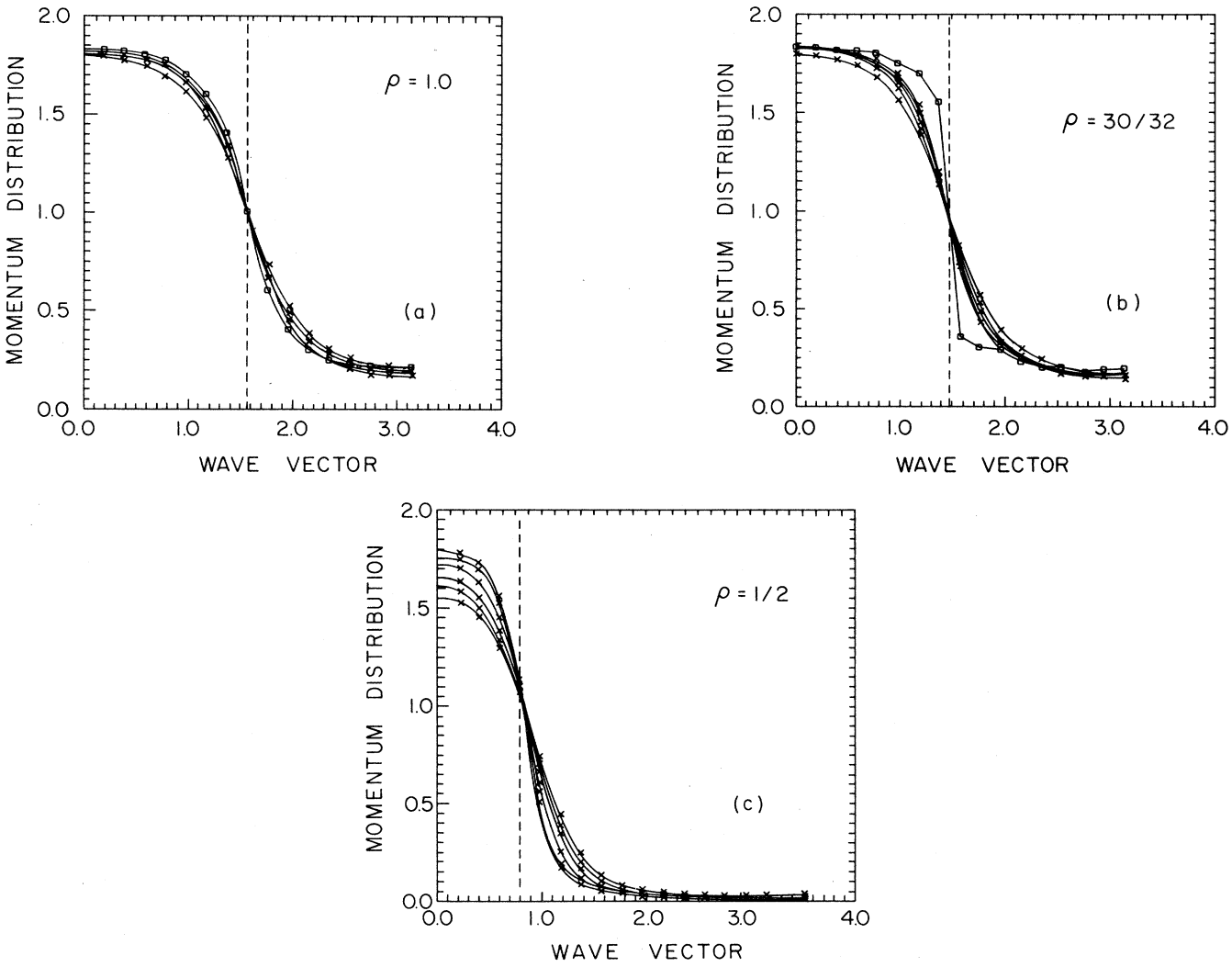

FIG. 4. Momentum distribution $n(k)=\langle c_{k_\uparrow}^\dagger c_{k_\uparrow}\rangle+\langle c_{k_\downarrow}^\dagger c_{k_\downarrow}\rangle$ for various band fillings and temperatures. In all cases, $L=32$, $t=1$, $U=4$. The imaginary-time step is $\Delta\tau=0.20$ in the quarter-filled case $\rho=\frac{1}{2}$; otherwise it is $\Delta\tau=0.125$. The solid lines are a cubic spline fit between the Monte Carlo results given by the crosses. (a) $\rho=1$, while $\beta=5$, 4.75, 4, 3.75, and 3. (b) $\rho=\frac{30}{32}$, while $\beta=5$, 4.75, 4, 3.75, and 3. (c) $\rho=\frac{1}{2}$, while $\beta=7$, 6, 5, 4, 3.75, 3.45, and 3. The largest quoted inverse temperatures β correspond to the largest values of the momentum distribution $n(k)$ to the left of the Fermi wave vector k_F (vertical dashed line), and to the smallest values to the right of that wave vector. The squares in the first two cases are the results of Ref. 1.

independent point at the free-electron value of the Fermi wave vector. This is in agreement with Luttinger's theorem,[10] and may be seen most easily by considering the following formula relating the momentum distribution and the spectral weight (in the isotropic-spin case):

$$n(k)\equiv\langle c^{\dagger}_{k_\uparrow}c_{k_\uparrow}\rangle+\langle c^{\dagger}_{k_\downarrow}c_{k_\downarrow}\rangle \equiv 2\int_{-\infty}^{+\infty}\frac{d\omega}{2\pi}\frac{A(k,\omega)}{e^{\beta(\omega-\mu)}+1}\ , \tag{2}$$

where the spectral weight $A(k,\omega)$ satisfies the sum rule

$$\int_{-\infty}^{+\infty}\frac{d\omega}{2\pi}A(k,\omega)=1\ . \tag{3}$$

When there exists a temperature-independent spectral weight in the low-temperature limit, and when this spectral weight is a δ function at a frequency $\omega=\mu$ for a value of k (the Fermi wave vector), then the momentum distribution is temperature independent at that wave vector. We now discuss in turn the results for each band filling.

A. Half filling

In the half-filled case, $\rho=1$, Fig. 4(a), our lowest-temperature results are consistent with the zero-temperature results of Ref. 1 indicated by squares. Clearly, then, this confirms that there is no Fermi surface in this case. This is also in agreement with results obtained from t/U expansions.[4] Note then that in this half-filled case, Luttinger's theorem in its original form does not hold since there is no jump in the momentum distribution (no Fermi surface). Nevertheless, $k=\pi/2$ remains an inflection point. Hence, the existence of a finite-temperature inflection point in the momentum distribution by itself cannot be taken as a proof of the existence of quasiparticles, but it is consistent with it, as discussed in the preceding paragraph.

B. Small hole doping near half filling

In the near half-filled case, $\rho=\frac{30}{32}$, Fig. 4(b), our results are inconclusive for reasons which we discuss momentarily. Around the Fermi wave vector, our results differ significantly from the zero-temperature results of Ref. 1 indicated by the squares. A possible source of difficulty is indicated by the small temperature dependence of the chemical potential seen in Fig. 3. This suggests that the low-temperature limit is not yet attained at the temperatures of interest. In other words, the convergence to the zero-temperature limit appears slower here than at half filling. Indeed, at the lowest temperature achieved ($\beta=5$), the band energy at the Fermi wave vector is within β^{-1} of the energy where Umklapp processes occur, suggesting that these processes are not completely frozen out, as they would be at sufficiently low temperatures. Another possible source of disagreement lies in the use of the grand-canonical ensemble in the present work, as opposed to the canonical one in Ref. 1. For finite systems, that difference may not always be neglected. The fluctuations in the number of particles, estimated from

$$\langle(\Delta N)^2\rangle=\frac{1}{\beta}\left[\frac{\partial N}{\partial\mu}\right]_T\ , \tag{4}$$

are between 3% and 4% in the present case. In the $\rho=1$ case, the same formula (4) gives fluctuations of order 2.5% at the highest temperature of Fig. 4(a) ($\beta=3$). Since the difference between the average band fillings $\rho=\frac{30}{32}$ and $\rho=1$ is about 6%, these fluctuations in the number of particles are appreciable.

C. Quarter filling

To understand the results for the quarter-filled band, it is best to recall, first, what is expected from the renormalization group. Straight perturbation theory is logarithmically divergent in one dimension, leading to spurious phase transitions. In the momentum-shell renormalization language of Wilson, one instead uses perturbation theory to eliminate large momenta, generating renormalized couplings.[2,8] Let g_1 be the vertex for backscattering, where two electrons on opposite sides of the Fermi surface exchange, and let g_2 be the vertex for forward scattering involving two electrons on opposite sides of the Fermi surface. Forward scattering for two electrons on the same side of the Fermi surface, g_4, is not directly involved in logarithmic divergences,[2] and so is neglected here. Umklapp terms, represented by g_3, also do not contribute at low temperature away from half filling. After eliminating the degrees of freedom in the curved sections of the dispersion relation for tight-binding bands, one is left only with the linear part of the dispersion relation around the Fermi surface. In this regime,[2,8] one obtains the following recursion relations for $\tilde{g}_i\equiv g_i/(\pi v_F)$:

$$\frac{d\tilde{g}_1}{dl}=-\tilde{g}_1^2\ , \tag{5a}$$

$$\frac{d\tilde{g}_2}{dl}=-\tfrac{1}{2}\tilde{g}_1^2\ , \tag{5b}$$

where l defines the cutoff energy through the relation

$$E(l)=E_c e^{-l}\ , \tag{6}$$

with E_c some bare cutoff of the order of the effective reduced bandwidth of the linear spectrum. Note that in reality the cutoff is defined in momentum space, but since the above-mentioned rescaling in the linear-band regime does not lead to Fermi velocity renormalization, one may interchangeably use energy or wave vector, both being linearly related through the initial Fermi velocity at E_c.

Most important for our purpose, the quasiparticle weight Z also obeys a recursion relation,

$$\frac{d\ln Z}{dl}=-\tfrac{1}{4}(\tilde{g}_1^2-\tilde{g}_1\tilde{g}_2+\tilde{g}_2^2)\ . \tag{7}$$

Note that $(\tilde{g}_1-2\tilde{g}_2)$ is a renormalization-group invariant. The large l solution of Eqs. (5) and (7) is then

$$Z(l)=C\left[\frac{E(l)}{E_c}\right]^{\theta}\ , \tag{8}$$

where C contains various constants of integration, and

$$\theta=\frac{1}{4}\left[\frac{\tilde{g}_1^0}{2}-\tilde{g}_2^0\right]^2=\frac{1}{4}\left[\frac{\tilde{g}_1^*}{2}-\tilde{g}_2^*\right]^2 . \tag{9}$$

Here, the superscript 0 represents initial condition, and the superscript $*$ the fixed point value.

As the cutoff goes to zero in Eq. (8), the quasiparticle weight also vanishes, as expected. However, finite temperature, or finite frequencies, set a minimal value of the cutoff. Under those conditions, one has a nonvanishing quasiparticle weight. In the present case, we are working in the limit

$$\Delta\epsilon=2t\sin k_F\Delta k\gtrsim\beta^{-1} , \tag{10}$$

where Δk is the difference between the last wave vector which can be eliminated and the Fermi wave vector, namely, $\Delta k=2\pi/L$, where $L=32$. The important conclusion, then, is that at sufficiently low temperatures, as defined by Eq. (10), the cutoff becomes $E_c(l)=\Delta\epsilon$ instead of temperature and hence the quasiparticle weight Z is determined through (10) and (8) by the system size. More specifically, under those conditions, Z vanishes as a power law of the system size, namely,

$$Z\approx L^{-\theta} . \tag{11}$$

The condition (10) also has another physically interesting interpretation in terms of length, namely, it can be rewritten as $\xi\gtrsim L$, where $\xi=2\pi v_F\beta$ is the thermal de Broglie wave length, which in this problem is the correlation length (defined with the Gaussian free-electron fixed point exponent).[8] For the simulation results to be discussed below, that length is 62 at the lowest temperature considered ($\beta=7$), and 27 at the highest one ($\beta=3$), which is indeed larger or of the order of the system sizes considered, $L=32$. Hence, it seems quite clear that our simulations, as well as those of Sorella *et al.* which are performed for $L=32$ and 200 with a zero-temperature algorithm, are in a regime where the quasiparticle jump at the Fermi surface is determined by the system size.

The result (11) may also be obtained from the following general finite-size scaling ansatz for the singular part of the momentum distribution:

$$n(k,T,L)=\lambda^{-\theta}N_{\pm}(|k-k_F|\lambda,T\lambda^{1/\nu},L/\lambda) , \tag{12}$$

where T is the temperature and N is a scaling function which is, in general, different for $k>k_F(+)$ and $k<k_F(-)$. At sufficiently small temperature, Eq. (12) predicts that for $|k-k_F|\gg L^{-1}$,

$$n(k,0,L)=|k-k_F|^{\theta}N_{\pm}(1,0,\infty) , \tag{13}$$

which is the usual result[2] for the zero-temperature momentum distribution in the thermodynamic limit, while for k just above (+) or just below (−) k_F,

$$n(k_F^{\pm},0,L)=L^{-\theta}N_{\pm}(0,0,1) , \tag{14}$$

as suggested by Eq. (11).

We use these results to interpret our simulations in the quarter-filled case $\rho=\frac{1}{2}$. While the temperature dependence of the momentum distribution in the $\rho=1$ and $\frac{30}{32}$ cases is too small compared with our Monte Carlo accuracy to allow us to extract information from that temperature dependence, in the case of $\rho=\frac{1}{2}$, as can be seen from Fig. 4(c), the temperature dependence of the momentum distribution is sufficiently large to allow us to perform the following approximate spectral analysis. In accordance with Eq. (11) and the preceding discussion, it is reasonable to fit our data by assuming that the spectral weight has a quasiparticle shape,

$$A(k,\omega)=2\pi\left[\frac{1-Z_k}{W}+Z_k\frac{\Gamma_k}{(\omega-\epsilon_k)^2+\Gamma_k^2}N_{k,\omega}\right]\theta(\omega-\omega_{\min})\theta(\omega_{\max}-\omega) , \tag{15}$$

where the first term represents a flat background with $W=\omega_{\max}-\omega_{\min}$ while the second term is a simple Lorentzian with a normalization factor

$$N_{k,\omega}=\frac{1}{\arctan[(\omega_{\max}-\epsilon_k)/\Gamma_k]-\arctan[(\omega_{\min}-\epsilon_k)/\Gamma_k]} , \tag{16}$$

which in practice is always close to unity for the W chosen and the Γ_k calculated. Equation (15) satisfies the sum rule (3) and is motivated by simplicity. Taking the spectral weight of Eqs. (15) and (16) to be independent of temperature, the three parameters, ϵ_k, Z_k, Γ_k, of Eqs. (15) and (16) are obtained by searching for the best fit of Eqs. (2), (15), and (16), to the temperature-dependent results of Fig. 4(c) for the momentum distribution. We took $\omega_{\min}=-2t$ and $\omega_{\max}=2t$ and verified that the results were independent of these bandwidth parameters, as long as they were a few Γ_k away from the quasiparticle energies.

The results for ϵ_k are illustrated by circles in Fig. 5. Note that for large values of k, the temperature dependence of the momentum distribution becomes comparable to, or smaller than, our Monte Carlo accuracy, preventing us to fit our results. The solid line is the curve,

$$\epsilon_k=-2t^*\cos k+\epsilon_0 , \tag{17}$$

with $\epsilon_0=0.31$ and $t^*=0.79$. Note that because the Monte Carlo results are nearly temperature independent at the Fermi wave vector, there one cannot obtain quasiparticle parameters by fitting the temperature dependence. Instead, the solid circle at the Fermi wave vector in Fig. 5 is, as one would expect from a simple quasiparticle model, simply at the coordinates $k_F=\pi/4$ and $\epsilon_k=\mu$ with μ the limiting low-temperature value of the chemical potential used in the simulation (see Fig. 3).

Solely from the fit, the uncertainties on the parameters

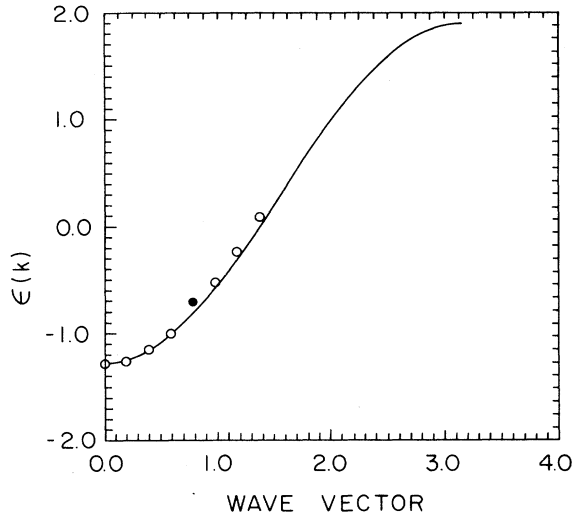

FIG. 5. Quasiparticle energy–wave-vector relation. Circles are obtained from a fit of the Monte Carlo data of Fig. 4(c) to Eqs. (2), (15), and (16). The solid line is the relation $\epsilon=-2t^*\cos k+\epsilon_0$ with $\epsilon_0=0.31$ and $t^*=0.79$. The solid circle is at $k_F=\pi/4$, $\epsilon_k=\mu=-0.71$. See text for a more complete discussion.

of Eq. (17) are of order $\Delta\epsilon_0=\pm0.05$ and $\Delta t^*=\pm0.02$. However, $t^*=0.79\pm0.02$ should not be used to estimate the renormalized Fermi velocity since there is no theoretical reason to fit the whole dispersion with the functional form of Eq. (17). Suppose for example that we restrict ourselves to wave vectors from 0 to k_F. With a maximum residual of 3%, that part of the dispersion may be fitted with $\epsilon_0=0.7$ and the bare value, t, of the hopping. Near the Fermi surface, we have basically only three points, including the Fermi wave vector, to find the effective Fermi velocity. Hence, a more realistic estimate of the Fermi velocity would yield, using only these points near the Fermi surface, $v_F^*=(0.85\pm0.15)v_F$.

The relative errors for ϵ_k are quite small, as can be seen from the smoothness of the results in Fig. 5. (The errors in v_F^* are much larger since they involve taking a derivative). For Z_k and Γ_k, the situation is less clear. Changes in Z_k and Γ_k to minimize χ^2, the mean-square difference between the fit and the data, are correlated: Larger Z_k and larger Γ_k may leave the χ^2 almost unchanged. Nevertheless, we can estimate that $\Gamma_k=0.03\pm0.02$ and $Z_k=0.95\pm0.05$, with a k dependence which is within the uncertainty. Near the Fermi surface, at $k=0.9817$, we obtained $\Gamma_k=0.005$, but we consider this to be within our uncertainty. As mentioned before, we cannot evaluate Γ_k at the Fermi surface itself. Note that even with Γ_k as large as 0.03, one would need extremely large system sizes to see zero-temperature rounding at the Fermi surface. Indeed, one can estimate that such rounding can be seen only when $\beta^{-1}<v_F\Delta k<\Gamma_k$ where, as above, $\Delta k=2\pi/L$, which implies, for $\Gamma_k=0.03$, system sizes larger than about 300.

As a final remark, note that since the widths Γ_k are much smaller than the smallest temperature considered $\beta^{-1}=\frac{1}{7}$, the frequency integral in Eq. (1) leads with great accuracy to the following functional form, which then also provides a reasonable fit to all the results of Fig. 4(c):

$$n(k)\equiv\langle c_{k_\uparrow}^\dagger c_{k_\uparrow}\rangle+\langle c_{k_\downarrow}^\dagger c_{k_\downarrow}\rangle=\frac{2Z}{e^{\beta(\epsilon_k-\mu)}+1}+B\ , \tag{18}$$

with ϵ_k given by Eq. (17) and with B a wave-vector-independent background. It turns out that if we allow a temperature dependence to Z, B, and t^*, this formula can also fit the results not only for $\beta>3$, but also for the high temperatures, from $\beta<3$ all the way to $\beta=\frac{1}{3}$ where the results are free-electron-like.

IV. DISCUSSION

Except very near half filling, where our results have not converged to the low-temperature limit, our simulations of the one-dimensional Hubbard model for $U/t=4$ confirm the results of Sorella *et al.*,[1] namely, at half filling, the numerical simulations are consistent with the absence of a Fermi surface even for relatively small system sizes, while at quarter filling, there is a Fermi surface in finite-size systems of order 32 sites. That the first result may be obtained for small systems simulations is easily understood from the strong localization which occurs at half filling. Our results have also shown that the zero-temperature limit is reached quite rapidly, a result which may be understood from the existence of a gap for that filling. We have seen that the second result, at quarter filling, is expected from the renormalization group in finite systems, as described more fully by the new scaling results Eqs. (11)–(14). The validity of the quasiparticle picture in finite systems has allowed us to extract the zero-temperature finite-size quasiparticle weight Z, even if our temperatures are not as low as those of Sorella *et al.* In fact, our finite-temperature analysis has allowed us to extract additional information, such as the dispersion relation. The long lifetime of quasiparticles all the way to the bottom of the band is an unexpected result. Clearly, however, the Fermi velocity which we obtained is that which is characteristic of finite systems at low temperatures, or of infinite systems at a temperature where the correlation length is of the order of the systems we have considered. Indeed, even if there is no renormalization of the Fermi velocity in the elimination of degrees of freedom steps, Fermi-liquid considerations lead to such a renormalization in the small cutoff theory. In that case, the Fermi velocity is related to the renormalized forward-scattering amplitudes by the usual Fermi-liquid relation.[11]

Finally, one should note that Sorella *et al.* also obtained a large Z even for systems of size 200. While that may seem surprising at first, this is in fact a consequence of the smallness of the exponent θ, a possibility which they also suggested. Indeed, from Eq. (11), we see that

$$Z(L=200)/Z(L=32)=(32/200)^\theta\ .$$

A very rough estimate for this exponent is obtained by setting $g_1^0=g_2^0=U$ and $v_F=2t\sin k_F$ in Eq. (9), from which one obtains $\theta=0.05$. Given that the dimensionless

couplings $\tilde{g}_1^0=\tilde{g}_2^0=U/(\pi v_F)$ are of order unity, this value can be considered as a lower bound in a perturbative renormalization-group procedure. However, even for θ twice as large, $\theta=0.1$, we obtain

$$Z(L=200)/Z(L=32)=0.83 .$$

Given our result $Z(L=32)\cong 0.95$, this is consistent with the result of Sorella *et al.*, $Z(L=200)\cong 0.8$. If corrections to scaling have not completely died out at $L=32$, $Z(L=200)$ would be predicted somewhat smaller. To our knowledge, the momentum-shell approach of Ref. 8 is the only one with which one could evaluate all the input parameters entering the determination of Z and of the renormalized coupling. Our preliminary estimates are consistent with the foregoing results. A more complete treatment of this is the subject of future work.

ACKNOWLEDGMENTS

We are indebted to Jean Vannimenus for the initial information and discussions which lead to this problem and to Laurent Caron for numerous enlightening discussions which were essential to the completion of this work. We are also indebted to Laurent Lewis for help with the supercomputing, and to A. Ruckenstein, R. Shankar, and R. M. Fye for discussions, and to P. Bénard, Rui Kan, and D. Vollhardt for pointing out various references. The support of the Natural Sciences and Engineering Research Council of Canada, and of the Ministère de l'éducation du Québec is gratefully acknowledged. A.-M.S.T. would like to thank the Steacie Foundation for support and the Institute for Theoretical Physics (ITP) for its hospitality during the writing of this work. The ITP is supported in part by the National Science Foundation under Grant No. PHY82-17853.

[1]S. Sorella, E. Tosatti, S. Baroni, R. Car, and M. Parrinello, Int. J. Mod. Phys. B **1**, 993 (1988); S. Sorella, S. Baroni, R. Car, and M. Parrinello, Europhys. Lett. **8**, 663 (1989).

[2]For an exhaustive review, see J. Sólyom, Adv. Phys. **28**, 201 (1979); V. J. Emery, in *Highly Conducting One-Dimensional Solids,* edited by J. T. Devresse, R. Pevrard, and V. E. van Doren (Plenum, New York, 1979).

[3]E. H. Lieb and F. Y. Wu, Phys. Rev. Lett. **20**, 1445 (1968); **21**, 192(E) (1968).

[4]J. Carmelo and D. Baeriswyl, Phys. Rev. B **37**, 7541 (1988); M. Takahashi, J. Phys. C **10**, 1289 (1977).

[5]J. E. Hirsch, Phys. Rev. B **31**, 4403 (1985); **28**, 4059 (1983); R. Blankenbecler, D. J. Scalapino, and R. L. Sugar, Phys. Rev. D **24**, 2278 (1981).

[6]J. E. Hirsch, R. L. Sugar, D. J. Scalapino, and R. Blankenbecler, Phys. Rev. B **26**, 5033 (1982); M. Barma and B. S. Shastry, *ibid.* **18**, 3351 (1978).

[7]J. E. Hirsch, Phys. Rev. B **38**, 12 023 (1988); S. R. White, R. L. Sugar, and R. T. Scalettar, *ibid.* **38**, 11 665 (1988); S. R. White, D. J. Scalapino, R. L. Sugar, E. Y. Loh, J. E. Gubernatis, and R. T. Scalettar, Phys. Rev. B **40**, 506 (1989).

[8]C. Bourbonnais, Mol. Cryst. Liq. Cryst. **119**, 11 (1985); Ph.D. thesis, Université de Sherbrooke, III-374, 1985.

[9]R. M. Fye, Phys. Rev. B **33**, 6271 (1986); R. M. Fye and R. T. Scalettar, *ibid.* **36**, 3833 (1987); M. Suzuki, Phys. Lett. **113A**, 299 (1985).

[10]J. M. Luttinger, Phys. Rev. **119**, 1153 (1960).

[11]A. A. Abrikosov, L. P. Gorkov, and I. E. Dzyaloshinski, *Methods of Quantum Field Theory in Statistical Physics* (Dover, New York, 1963), pp. 161–163.